EFFECT OF IMPURITIES UPON THE NUCLEATION OF DISLOCATION LOOPS IN QUENCHED ALUMINUM

by

R. J. DiMelfi and R. W. Siegel

Department of Materials Science
State University of New York at Stony Brook
Stony Brook, L. I., New York

College of Engineering
Report #181
October, 1970

EFFECT OF IMPURITIES UPON THE NUCLEATION OF DISLOCATION LOOPS IN QUENCHED ALUMINUM †

by

R. J. DiMelfi and R. W. Siegel

Department of Materials Science
State University of New York at Stony Brook
Stony Brook, L.I., New York

ABSTRACT

The effect of pre-quench annealing in air upon vacancy precipitation in quenched aluminum of nominal 99.9999 wt. % purity was studied. Aluminum ribbons were resistance heated for varying lengths of time in air at 600°C and subsequently quenched from 580°C into a controlled bath at 40°C in which the vacancy precipitation proceeded to completion. The electrical resistivity at 4.2°K was then measured for each specimen and compared with its value measured prior to the quench. The specimens were investigated by transmission electron microscopy in order to directly observe the resultant vacancy precipitate ensemble. It was found that the faulted dislocation loop density decreased monotonically with increasing duration of the pre-quench anneal, t_a. However, the pre-quench bulk resistivity ratio, $\rho(20^{\circ}C)/\rho(4.2^{\circ}K)$, of the specimens was found to be independent of t_a, except in a preliminary period of annealing, with a value of 2309±62. It is concluded that the dislocation loops were nucleated heterogeneously at impurity sites over the range of specimen purity investigated. The results are interpreted on the basis that the concentration of impurities

---

† This work was supported by the National Science Foundation under Grant No. GK-3435.

active in the dislocation loop nucleation process was reduced during the pre-quench anneal, but that this variation in impurity concentration was small enough to be undetectable in the resistivity ratio measurements. In addition, a value for the stacking fault resistivity at $4.2^{o}K$ in aluminum, $\rho_{SF} = (3.2 \pm 1.1) \times 10^{-13}\ \Omega\ cm^2$, was determined. The results of the present investigation are discussed in relation to previous work.

1. INTRODUCTION

The vacancy precipitate structure in quenched and aged nominally pure aluminum has been widely studied using transmission electron microscopy. It has been generally established that the vacancy precipitates formed are dislocation loops of the Frank sessile type containing stacking faults (hexagonal loops on (111) planes with [110] edges) and octahedral voids with (111) faces (Yoshida et al. 1963a, Cotterill and Segall 1963, Kiritani and Yoshida 1963, Kiritani 1964). The relative densities of these two types of vacancy precipitates has been found to depend strongly upon a number of quenching variables (Kiritani 1964, Yoshida et al. 1965b, Shimomura and Yoshida 1967) such as specimen purity, quenching rate and aging temperature.

Investigations of the effect of purity upon the vacancy precipitates formed in quenched aluminum have been carried out. Cotterill and Segall (1963) and Cotterill (1965) attempted to correlate specimen purity with the nature of the vacancy defects produced upon quenching and aging. In the former work, further purification of initially 99.995 wt. % pure aluminum was accomplished during the process of multiple quenching. A decrease in the dislocation loop density, accompanied by an increase in

loop size, was observed for the specimens of higher purity. More recent studies (discussion of Cotterill 1965, Førsvoll 1965) have indicated that the successive air annealing between the quenches was most likely responsible for their observed purifying effect. Yoshida, et al. (1963a) studied the effect of specimen purity upon vacancy condensation using specimens of four nominal purity levels ranging from 99.995 wt. % to about 99.9999 wt. % pure aluminum. It was observed that, for the same quenching and aging conditions, the dislocation loop density decreased, while the loop size increased, for successively purer specimens. Shimomura and Yoshida (1967) quenched aluminum of three nominal purities, 99.995 wt. %, 99.999 wt. % and zone refined (∿ 99.9999 wt. %), from various atmospheres and observed the resulting vacancy precipitates. Their experimental results regarding dislocation loop densities in specimens quenched after annealing in air for 10 h at 620°C were generally in accord with the previous investigations showing a decrease of loop density with increasing specimen purity. However, voids were observed along with the dislocation loops in specimens which were pre-quench annealed in either hydrogen or in air containing normal amounts of water vapor. It was concluded that dissolved hydrogen atoms provided heterogeneous nucleation sites for the voids. It was also found that the formation of voids was strongly suppressed in less pure aluminum which had been annealed in wet air, presumably due to the enhanced nucleation of dislocation loops in the more impure specimens. In a subsequent investigation (Sato et al. 1967) a comparison was made between the vacancy precipitates in quenched and aged nominally 99.999 wt. % pure aluminum specimens which were degassed and those in specimens which were quenched from wet air in the standard manner. It was found that the density of dislocation loops observed was essentially

unaffected by the simultaneous formation of voids, the only effect being the reduction of the final size of the loops when voids were present due to the competition for the precipitating vacancies between the loops and voids.

Ytterhus and Balluffi (1965) observed a decrease in the dissolved impurity content of initially 99.999 wt. % pure gold after pre-quench annealing in air in the temperature range from 850°C to 1000°C. This effect was monitored by measuring the ratio of the electrical resistance at room temperature to that at liquid helium temperature, $R(24^{\circ}C)/R(4.2^{\circ}K)$, which increased with increasing duration of annealing in air. The high temperature anneal also had a marked effect upon the subsequent annealing kinetics of the quenched-in vacancy defects. Siegel (1966a, b) similarly purified gold specimens of 99.999 wt. % and 99.9999 wt. % nominal purity, and determined the effect of this further purification upon the vacancy annealing kinetics and upon the vacancy precipitate structure in quenched and aged foils by direct observation in the electron microscope. A monotonic decrease in the vacancy precipitate density, with a concomitant increase in precipitate size, was observed with increasing specimen purity. It was concluded that vacancy precipitates nucleated heterogeneously at impurity sites over the whole range of purity studied. A similar refining effect has been observed in aluminum after annealing in air at elevated temperatures (Førsvoll 1965, Førsvoll and Foss 1967). An investigation into the effect of such further purification of initially 99.9999 wt. % pure aluminum upon the vacancy precipitate structure, after quenching and aging, has not previously been made.

The disappearance of vacancy precipitates has been shown to be responsible for the decrease in resistivity during the second stage of iso-

chronal annealing in quenched aluminum (Cotterill 1963). Hence, if the difference in resistivity between the quenched-and-aged state and the fully annealed condition of a specimen which contained only faulted dislocation loops is measured, the contribution to the resistivity due to the presence of these vacancy precipitates can be determined. This precipitate resistivity consists of contributions from both the stacking faults and the dislocation lines comprising the faulted loops. If the part attributed to the dislocation lines can be separated from the total quantity, a value of the stacking fault resistivity, ρ_{SF}, in aluminum can be obtained. Such measurements of the stacking fault resistivity in aluminum at 78°K have been made (Kino et al. 1963, Yoshida et al. 1963b, 1965b), but a value of ρ_{SF} at 4.2°K in aluminum has not previously appeared in the literature.

In the light of the above information, it was decided to conduct an investigation of the effect of further purification by air annealing upon the vacancy precipitate structure of quenched and aged nominal high purity aluminum. It was hoped that such an investigation would provide information regarding the dislocation loop nucleation process in this upper region of purity in aluminum and would increase our understanding of the role which impurities play in the nucleation of vacancy precipitates in metals. In addition, a measurement of the stacking fault resistivity, ρ_{SF}, at 4.2°K in aluminum could be obtained.

2. EXPERIMENTAL PROCEDURE

2.1. Specimen Material and Purity

The material used in the present investigation was initially 99.9999 wt. % pure polycrystalline aluminum foil supplied by Cominco American,

Inc. An analysis of the supplied material is presented in table 1. The specimens furnished were ribbon-shaped, approximately 18 cm long, 0.089 cm wide and 0.017 cm thick. The foils were annealed in air at (600 ± 5)^{o}C for varying lengths of time in order to decrease the dissolved impurity content (Førsvoll, 1965). The ratio of the room temperature resistivity to that at liquid helium temperature, $\rho(20^{o}C)/\rho(4.2^{o}K)$, was measured in an attempt to monitor the purifying effect.

2.2. Quenching and Resistivity Measurements

The aluminum ribbons were shaped into standard quenching specimens and mounted on light copper frames. The shape of the specimens and design of the frames were similar to those used by Ytterhus and Balluffi (1965). Potential leads made of 0.005 cm diameter aluminum wire, supplied by the Sigmund Cohn Corporation, were spot welded to the specimens at points separated by a gauge length of approximately 4 cm. The specimens were carefully cleaned in a 50% nitric acid solution, and rinsed in distilled water followed by methanol. They were then d. c. resistance heated at approximately 560^{o}C for one hour, while the specimen shape was altered slightly in order to obtain an even temperature distribution along the gauge length. The temperature variation along the wires was measured with an Ircon Infrared Radiation Thermometer, and was found to be within ± 1%. In order to avoid specimen contamination during the heating cycles, the wires were always carefully cleaned prior to each of these treatments. The pre-quench annealing temperature and the quenching temperature were determined by measuring the ratio of the electrical resistance of the specimen at temperature to that measured at 20^{o}C and using the temperature dependence of the resistance of aluminum as measured by Simmons and

Balluffi (1960). The resistance of the specimens at 20°C was measured using standard potentiometric techniques before and after the pre-quench anneal. The value of $R(20^{o}C)$ measured before the pre-quench anneal was used to set the pre-quench annealing temperature, T_a, while that measured after the anneal was used to set the quenching temperature, T_Q, and to compute the resistivity values at 4.2°K.

Six specimens were d. c. resistance heated at $T_a = (600 \pm 5)^{o}C$ for 0 h, 5 h, 20 h, 23 h, 36 h, and 48 h, respectively. The resistance of each of the specimens was measured at 4.2°K after this pre-quench anneal and a resistivity ratio, $\rho(20^{o}C)/\rho(4.2^{o}K)$, was determined in order to obtain an indication of its relative purity level. Resistivity values were obtained from the resistance measurements at 4.2°K using the relation

$$\rho(4.2^{o}K) = [R(4.2^{o}K)/R(20^{o}C)]\ \rho(20^{o}C)$$

and the value for the resistivity of aluminum at 20°C, $\rho(20^{o}C) = 2.641 \times 10^{-6}\ \Omega$ cm, determined by Førsvoll and Foss (1967).

After the resistivity ratio was obtained, the specimen was placed approximately 1 cm above the surface of the quenching medium (distilled water) in a draft free quenching bath. The specimen was oriented relative to the liquid surface in such a way that the entire gauge length would enter the quenching medium simultaneously. Care was also taken to insure that the ribbon entered the water edgewise in order to avoid deformation. The specimen was then resistance heated to the quenching temperature, $T_Q = (580 \pm 5)^{o}C$, held there for a time no greater than 10 min, in order to minimize any further high temperature refining, and rapidly ($>10^{4}$ °C/sec) quenched into the distilled water held at

40°C. The heating current was turned off only after the specimen had entered the water in order to avoid the specimen temperature decrease prior to entering the quenching medium inherent in furnace quenching techniques. The specimens were then fully aged in situ at T_A = (40.00 ± 0.05)°C, in the same constant temperature bath. The quenching and aging conditions were specifically chosen to produce fairly large faulted dislocation loops while minimizing the formation of voids (Kiritani 1964, Yoshida et al. 1965b). After aging was complete, the specimen resistivity at 4.2°K, $\rho(\infty)$, was determined. A Honeywell six-dial potentiometric system was used for the resistance measurements at 4.2°K, which provided a sensitivity of ± 1 x 10^{-12} Ω cm.

2.3. Direct Observation of Precipitate Structure

After the final resistivity measurement was made, the specimen was removed from the copper frame and the gauge length was cut from the specimen. This procedure was carried out with extreme care in order to avoid deformation of the specimen. Shimomura (1965) has pointed out that a slight amount of deformation can be responsible for the unfaulting of a large number of dislocation loops. The specimens were subsequently electro-thinned from one end using a window method and a standard electrolyte consisting of an 80% ethanol and 20% perchloric acid solution. Thin foil samples were always obtained well away from the cut edge of the specimens, thus avoiding any perturbation to the vacancy precipitate structure in that area. The electron microscopy samples were observed in transmission at 100 kv in a Philips Model EM 300 electron microscope, fitted with a goniometer stage and a rotation specimen holder. Since dislocation loop loss from thin foils can occur due to stresses resulting from con-

tamination in the microscope, an anti-contamination device was employed during all electron microscopy observations.

The vacancy precipitate structure was examined on electron micrographs with a magnification of 25,000 x. Thin foil samples were taken from fairly well separated points on each specimen and several micrographs were taken of the regions of uniform loop density in each. Each micrograph was accompanied by an electron diffraction pattern indicating the crystal orientation of the corresponding area. The counting of the dislocation loops in the micrographs was done with a Zeiss Particle Size Analyzer. Three or more samples were taken from each specimen and approximately 300 loops were counted on each sample.

Since there were four possible (111) planes on which the loops could be oriented, there were in general four different projections of the perfect hexagonal precipitates on the plane of the foil. In counting, the largest loop diameter projected in the foil plane was measured. This diameter was resolved onto the proper (111) plane and in the correct [110] direction to give the actual size of the loops. The root-mean-square diameter, d_{rms}, of the loops of a particular specimen was then determined.

In order to obtain the precipitate densities, foil thicknesses were obtained from the width of slip traces (Hirsch et al. 1965). However, two factors had to be considered when computing the dislocation loop densities from the electron micrographs. First, if a set of loops, with Burgers vector $\vec{b}$, is oriented such that $\vec{g} \cdot \vec{b} = 0$ (where $\vec{g}$ is the operating reflection vector) then these loops will not be observed (Hirsch et al. 1960) giving an apparent loop density less than that actually present. This problem was eliminated in the present investigation by tilting the

areas under observation until a maximum loop density came into contrast so that four distinct loop orientations, corresponding to the four unique (111) planes, were observed in all of the thin foil samples examined (see for example fig. 2). Second, a correction of the measured foil thickness, t, was required due to the presence of denuded regions near the foil surfaces which are formed as a result of the loss of any dislocation loop which intersects the surface. An effective thickness, t_{eff}, was obtained by subtracting from the measured thickness, t, the projection of the loop radius, $d_{rms}/2$, onto the normal to the foil surface for the two surfaces. Thus,

$$t_{eff} = t - d_{rms} \sin \theta \quad ,$$

where θ is the angle between the specific (111) plane in which the hexagonal faulted loop lies and the plane of the foil. Therefore, for each loop orientation there is a corresponding effective thickness. The total density of faulted loops, then, is the sum of the four densities computed for each of the loop orientations. It was found that the individual density from each orientation was approximately ¼ of the total density, N_s, within reasonable uncertainty limits. This observation indicates that the faulted loops were randomly distributed on the four (111) planes and that there was no preferential loop loss from any particular (111) plane.

In observing the precipitate structure, regions near grain boundaries and dislocation networks were avoided so that the results would be representative of the unperturbed bulk crystal. In general, the size and density of the precipitate structure was obtained with good uniformity.

2.4. Summary

In summary, six 99.9999 wt. % pure aluminum specimens, numbered one through six, were annealed in air at $T_a = (600 \pm 5)^{\circ}C$ for 0 h, 5 h, 20 h, 23 h, 36 h, and 48 h, respectively. The resistivity ratio, $\rho(20^{\circ}C)/\rho(4.2^{\circ}K)$, was determined for each. The specimens were then rapidly quenched from $T_Q = (580 \pm 5)^{\circ}C$ into distilled water at $T_A = (40.00 \pm 0.05)^{\circ}C$ and fully aged at that temperature in the same bath. The resistivity at $4.2^{\circ}K$ was subsequently measured ($\rho(\infty)$). Transmission electron microscopy samples were then prepared, and the vacancy precipitate structure was observed.

3. RESULTS

3.1. Resistivity Ratio

The pre-quench annealing time, t_a, ranging from 0 h to 48 h at $600^{\circ}C$ was measured starting after a one hour anneal at $\sim 560^{\circ}C$, during which time adjustments were made on the specimen temperature distribution (see section 2.2.). The effect of annealing in air upon the purity (dissolved impurity content) was monitored by measuring the resistivity ratio, $\rho(20^{\circ}C)/\rho(4.2^{\circ}K)$, after each pre-quench anneal. A plot of the results of these measurements (fig. 1) shows that the resistivity ratio remained essentially constant, with an observed mean value of 1968 ± 53, over the entire range of annealing times. This measured mean resistivity ratio corresponds to a bulk resistivity ratio of 2309 ± 62 obtained by correcting for the effect of specimen size.† The observed constancy of the resistivity ratio indicates that any further purification of these

---

† This correction was calculated using the theory of Sondheimer (1952) in the limit of diffuse surface scattering and the measured value of the product $\rho_o\lambda_o = 7.0 \times 10^{-12}\ \Omega\ cm^2$ (Førsvoll and Holwech, 1963) for aluminum, where ρ_o is the bulk resistivity and λ_o is the bulk electron mean free path.

specimens caused by the heating in air was not reflected in the resistivity ratio, for the range of t_a studied and with the sensitivity of the present resistivity measurements.

A seventh specimen, which received no heat treatment other than a 30 min anneal at 350°C to eliminate dislocations introduced by shaping, had a measured resistivity ratio of 1720. This specimen was then annealed for 3 h at (600 ± 5)°C and the measured resistivity ratio increased to 2035. Further annealing at 600°C resulted in normal scatter about the mean value of 1968 ± 53 for annealing times up to 33 h. These results (also plotted in fig. 1) seem to indicate that the air annealing did have some effect upon $\rho(20^{\circ}C)/\rho(4.2^{\circ}K)$ very early in the process for the material used in the present investigation. This increase in the resistivity ratio can be attributed to the removal of dissolved impurities, since it could not have been caused by further dislocation annealing (Clarebrough et al. 1961, Basinski et al. 1963).

3.2. Observed Precipitate Structure

Figure 2 contains two electron micrographs showing the typical precipitate structures observed. The specimens from which these samples were taken were given a pre-quench anneal at 600°C for times of t_a = 0 h for fig. 2(a) and t_a = 23 h for fig. 2(b). It can be seen that the observed vacancy precipitates were hexagonal faulted dislocation loops on (111) planes. No other types of vacancy precipitates, such as voids, were observed in any of the foils examined from specimens 1-5 (0 h $\leq t_a \leq$ 36 h) even though they were carefully looked for. An exception to this was a small number of double layer faulted loops (Yoshida et al. 1965a, Kiritani 1965) observed in the specimens with longer pre-quench annealing times,

t_a (as shown in fig. 2(b)). Among these specimens, an increasing number of double layer faulted loops (up to $\sim$ 5% of the loops) was observed with increasing t_a. In specimen 6 (t_a = 48 h), however, voids were observed in addition to the dislocation loops while a negligible number (< 1%) of double layer faulted loops were found. The void density and mean size observed in this specimen were $N_v \simeq 2.4 \times 10^{14}$ cm^{-3} and $\ell_v \simeq 75$ Å, respectively.

The electron microscopy data concerning the dislocation loops for the six specimens are presented in table 2, where t_a is the pre-quench annealing time at 600°C, N_s is the dislocation loop density and d_{rms} is the root-mean-square loop diameter. Also tabulated are the stacking fault area density, $A_{SF} = (3\sqrt{3}/8)\, d_{rms}^{\ 2} N_s$, the dislocation line length density of the loops, $\ell_{disl} = 3\, d_{rms} N_s$, and the vacancy concentration stored in the loops, $c_v = a_o A_{SF}/\sqrt{3}$, where a_o is the lattice parameter of aluminum (a_o = 4.05Å). The uncertainty in the values tabulated is given by the mean deviation in all cases.

It can be seen from table 2 that the value of c_v was essentially constant for specimens 1-5. Furthermore, for specimen 6 the sum of the concentration of vacancies stored in the observed voids, c_v (voids) = $(\sqrt{2}/3)\, \ell_v^{\ 3} N_v \simeq 0.5 \times 10^{-4}$, and that stored in the dislocation loops (see table 2) closely agrees with the value of c_v for the other specimens. The mean value obtained for the quenched-in vacancy concentration, assumed to be equal to the concentration of vacancies stored in the observed precipitates was $\bar{c}_v = (1.1 \pm 0.1) \times 10^{-4}$, indicating a constant quenched-in vacancy concentration for the six specimens. This value for $\bar{c}_v$ is in reasonable agreement with that determined from the quenching data of Bass (1967) by extrapolating his plot of quenched-in resistivity ($\Delta\rho_Q$) vs.

T_Q^{-1}, for a brine quench, to $T_Q = 580^oC$, and using the value of the vacancy resistivity, $\rho_v = (2.5 \pm 0.8) \times 10^{-6}$ Ω cm/at.% vacancies, obtained by Kabemoto (1965).

Figure 3 is a plot of the observed dislocation loop density, N_s, versus pre-quench annealing time, t_a. From this graph, it can be seen that the density of faulted loops decreased monotonically with increasing time. It should be emphasized that the quenching and aging conditions were kept fixed for all six specimens, resulting in a constant quenched-in vacancy concentration, and the only quantity varied was the pre-quench annealing time.

3.3. Stacking Fault Resistivity

The resistivity of the specimens was measured at 4.2^oK before quenching, $\rho(4.2^oK)$, and after the vacancy precipitation process was completed, $\rho(\infty)$. The residual resistivity increment, $\Delta\rho(\infty)$, due to the presence of the vacancy precipitates was thus obtained by taking the difference between these two values,†

$$\Delta\rho(\infty) = \rho(\infty) - \rho(4.2^oK) \quad ,$$

since $\rho(4.2^oK)$ was the base residual resistivity for the well annealed material. The measured values of $\rho(4.2^oK)$ and $\Delta\rho(\infty)$ for the six specimens are presented in table 2.

An upper limit to the stacking fault resistivity, ρ_{SF}, at 4.2^oK in aluminum may be obtained from the present data by simply dividing the measurements of $\Delta\rho(\infty)$ in the specimens containing only faulted dislocation loops (1-5) by the respective values of A_{SF} and averaging, if it is

---

† The resistivity size effect correction to $\Delta\rho(\infty)$ is negligible for these specimens.

assumed that the contribution to $\Delta\rho(\infty)$ from the dislocation loop lines is negligible. An upper limit, computed in this manner, was found to be $\rho_{SF}(4.2^{o}K) < (3.6 \pm 1.1) \times 10^{-13}\ \Omega\ cm^{2}$. A more exact estimate of ρ_{SF} can be obtained by taking into account the dislocation contribution to the vacancy precipitate resistivity, $\Delta\rho(\infty)$. If it is assumed that one can simply sum the stacking fault and dislocation contributions to the resistivity, then

$$\Delta\rho(\infty) = \rho_{SF}A_{SF} + \rho_{d}\ell_{disl} \quad ,$$

where ρ_{d} is the resistivity of the dislocations and the other parameters are as defined previously. The stacking fault resistivity is then given by

$$\rho_{SF} = \frac{\Delta\rho(\infty)}{A_{SF}} - \rho_{d}\left(\frac{\ell_{disl}}{A_{SF}}\right) . \qquad (1)$$

All of the parameters in eqn. (1) have been measured in the present experiment except ρ_{d}. Due to both scatter in the measured $\Delta\rho(\infty)$ values and the limited range of observed ℓ_{disl}, an adequate value of the dislocation resistivity could not be obtained from the present data. In lieu of this, an estimate can be made of the dislocation contribution to the faulted loop resistivity at $4.2^{o}K$ by using an appropriate value of ρ_{d}. Yoshida et al. (1965b) determined an upper limit for ρ_{d} from faulted loops in quenched aluminum at $78^{o}K$ and found $1.5 \times 10^{-19}\ \Omega\ cm^{3}$, while Rider and Foxon (1966) measured the dislocation resistivity in lightly cold-worked aluminum and obtained $(2.9 \pm 0.4) \times 10^{-19}\ \Omega\ cm^{3}$ at $\sim 78^{o}K$ and $(1.8 \pm 0.1) \times 10^{-19}\ \Omega\ cm^{3}$ at $4.2^{o}K$. While none of these values is exactly appropriate in terms of both dislocation type and temperature of measurement for the present computation, the ρ_{d} measured by Yoshida

et al. (1965b) was used, along with the data in table 2 for specimens 1-5, to obtain ρ_{SF} from eqn. (1). In this manner, an average value for the stacking fault resistivity at 4.2°K in aluminum

$$\rho_{SF}(4.2^{\circ}K) = (3.2 \pm 1.1) \times 10^{-13}\ \Omega\ cm^2$$

was obtained. Since the dislocation contribution to the faulted loop resistivity was small (∿11%) compared with that from the stacking fault, the exact choice of ρ_d was in fact not critical.

4. DISCUSSION

4.1. Effect of Air Annealing upon the Resistivity Ratio, Purity, and Precipitate Structure

It has been shown (Førsvoll 1965, Førsvoll and Foss 1967) that high temperature annealing in air can increase the electrical conductivity of aluminum by the diffusion of impurities (magnesium and possibly others) to the surface of the specimens. This purification, as one would expect, was found to vary with both specimen thickness and initial purity. Førsvoll and Foss (1967) found that the resistivity ratio, $\rho(20^{\circ}C)/\rho(4.2^{\circ}K)$, increased by a factor of three after annealing 0.016 cm thick specimens of "commercial super purity" aluminum with initial resistivity ratios of 500 for 50 h at 600°C. However, for specimens of zone-refined aluminum with resistivity ratios of 10,000 no changes were observed. The results of the resistivity measurements in the present investigation, therefore, appear to be consistent with the observations of Førsvoll and Foss (1967), where the purity of the present specimens lies for the most part in a range in and above which the purifying effect of high temperature air annealing cannot be monitored by resistivity ratio measurements with the present sensitivity.

The observed monotonic decrease of dislocation loop density, N_s, with increasing duration of pre-quench anneal, t_a, for fixed quenching and aging conditions, however, indicates that loop nucleation was made increasingly more difficult by this annealing. Further evidence for this is the observation of an increased incidence of double layer faulted loops, which have been shown to form by the successive nucleation of dislocation loops (Yoshida et al. 1965a, Kiritani 1965), in specimens with longer pre-quench anneals. Previous work (Shimomura and Yoshida 1967) has shown that the formation of voids in aluminum quenched from wet air is more likely when dislocation loop nucleation is difficult (as in their purer specimens). Thus, it appears likely that the presence of voids in specimen 6 (t_a = 48 h) was a consequence of the difficulty of loop nucleation in this specimen. Sato et al. (1967) have observed that the density of faulted loops is, however, essentially unaffected by void formation, but that the final loop size is reduced by the competitive loss of vacancies to the voids. This is consistent with the data presented in table 2, where it can be seen that while the loop density, N_s, continuously decreases with t_a, the loop size, d_{rms}, continuously increases for specimens 1-5, but then becomes considerably smaller in specimen 6 which also contained voids. Therefore, while the void formation in specimen 6 did not apparently affect the loop density in this specimen, their presence and that of the double faulted loops in the specimens with longer t_a were an additional manifestation of the increased difficulty with which the faulted dislocation loops were nucleated in the specimens with a longer pre-quench anneal. Under the fixed quenching and aging conditions of the present experiment, if the nucleation of faulted dislocation loops occurred homogeneously (i.e., only by vacancy-vacancy interactions), then

the density and size of the loops should have remained essentially unchanged from one specimen to another. If, however, the nucleation process occurred heterogeneously at impurity sites, and the high temperature pre-quench anneal removed such dissolved impurities from the bulk, the size and density of the precipitates should have been affected by the length of time, t_a, at 600°C. It appears evident from the decrease of N_s by a factor of three, with a concomitant increase in d_{rms}, as t_a varied from 0 h to 48 h that impurity nucleation sites for vacancy precipitation in the form of faulted dislocation loops were removed by the high temperature air annealing, resulting in the observed changes in the precipitate ensemble.

The observation that the resistivity ratio showed no change over the entire 48 h range of annealing times at 600°C is not inconsistent with this conclusion. If one assumes only one active impurity site per vacancy precipitate, the decrease in N_s observed could be accounted for by a decrease in the concentration of active impurities of approximately 6×10^{-10}. This change would result in a corresponding decrease in the resistivity at 4.2°K, assuming a resistivity for the active impurity of 2 μΩ cm/at.% (Blatt and Frankhauser 1966), of 1.2×10^{-13} Ω cm, or by almost an order of magnitude less than the sensitivity limits ($\sim \pm 1 \times 10^{-12}$ Ω cm) of the measuring apparatus used, and more than two orders of magnitude less than the mean deviation ($\sim \pm 4 \times 10^{-11}$ Ω cm) of the $\rho(4.2^{\circ}K)$ measurements. It is therefore not at all inconsistent that no change in the resistivity ratio was detected while a change of a factor of three in the loop density was observed. It should be pointed out however, that the resistivity measurements were sufficiently sensitive

to preclude an interpretation of the observed changes in the precipitate structure as being due to the introduction of impurities during air annealing which might act as shallow trapping sites for the vacancies, thereby altering the precipitate nucleation characteristics. If one takes even a very small impurity resistivity of 0.2 μΩ cm/at.%, any undetected increase in impurity concentration would have been less than 2×10^{-6}, as compared with the quenched-in vacancy concentration of 1.1×10^{-4}.

The results of the present investigation can thus be explained in the following way. During the earliest stages of pre-quench air annealing, while impurity concentration gradients were sufficiently high, the decrease in dissolved impurity content was large enough to affect $\rho(4.2^{\circ}K)$. Later, as the rate of removal of impurities decreased, the decrease in impurity content was too small to be reflected in the $\rho(4.2^{\circ}K)$ measurements. However, the nucleation of the vacancy precipitates, being very sensitive to small changes in the concentration of active impurities, was affected by the pre-quench anneal over the entire time range. Since the quenching and aging conditions were kept constant for all six specimens, and only the pre-quench annealing time was varied, the monotonic decrease in N_s indicates that the faulted dislocation loop nucleation occurred heterogeneously at impurity sites in this high purity range. This conclusion is consistent with the results of previous investigations (Yoshida, et al. 1963a, Shimomura and Yoshida 1967, Kiritani et al. 1969) which have compared the formation of dislocation loops in quenched aluminum of different nominal purities. The question of which specific impurities provide the dislocation loop nucleation sites, however, remains unanswered. These observed results and conclusions regarding vacancy precipitate nucleation in high purity aluminum are also consistent with the results of similar work on high purity gold (Siegel 1966a).

4.2. Stacking Fault Resistivity

The most reliable of the previous measurements of the stacking fault resistivity in aluminum, all at 78°K, appears to be that by Yoshida et al. (1965b). The individual contributions to the total vacancy precipitate resistivity from voids, stacking faults and dislocation loop lines were determined by using different quenching and aging conditions (Kiritani 1964) in order to vary the ensemble of vacancy precipitates. A value for $\rho_{SF}(78^{\circ}K) = (4.0\pm1.5) \times 10^{-13}$ Ω cm^2 was obtained. The very large value of $\rho_{SF}(78^{\circ}K) = 2 \times 10^{-12}$ Ω cm^2 reported by Kino et al. (1963) was most likely a result of the difficulties inherent in combining their resistivity measurements with electron microscopy data from another work (Yoshida et al. 1963a). The value of the stacking fault resistivity in aluminum at 4.2°K determined in the present investigation, $\rho_{SF}(4.2^{\circ}K) = (3.2\pm1.1) \times 10^{-13}$ Ω cm^2, is seen to be in reasonable agreement with that measured at 78°K by Yoshida et al. (1965b). While the ∿25% larger value obtained at 78°K may represent a reasonable deviation from Matthiessen's Rule in the range 4.2°K to 78°K for the stacking fault resistivity in aluminum, such a conclusion cannot be drawn with any degree of certainty due to the difficulty of comparing such independent measurements. The present determination of $\rho_{SF}(4.2^{\circ}K)$ compares favorably with a theoretical estimate (1×10^{-13} Ω cm^2) made by Howie (1960).

REFERENCES

Basinski, Z. S., Dugdale, J. S., and Howie, A., 1963, Phil. Mag. 8, 1989.

Bass, J., 1967, Phil. Mag. 15, 717.

Blatt, F. J. and Frankhauser, H. R., 1966, Calculations of the Properties of Vacancies and Interstitials (NBS misc. publ. 287), U. S. Government Printing Office, Washington, 109.

Clarebrough, L. M., Hargreaves, M. E., and Loretto, M. H., 1961, Phil. Mag. 6, 807.

Cotterill, R. M. J., 1963, Phil. Mag. 8, 1937.

Cotterill, R. M. J., 1965, Lattice Defects in Quenched Metals, edited by R. M. J. Cotterill et al., Academic Press, New York, 97.

Cotterill, R. M. J. and Segall, R. L., 1963, Phil. Mag. 8, 1105.

Førsvoll, K., 1965, Phil. Mag. 11, 419.

Førsvoll, K. and Foss, D., 1967, Phil. Mag. 15, 329.

Førsvoll, K. and Holwech, I., 1963, J. App. Phys. 8, 2230.

Hirsch, P. B., Howie, A., Nicholson, R. B., Pashley, D. W., and Whelan, M. J., 1965, Electron Microscopy of Thin Crystals, Butterworths, London, 418.

Hirsch, P. B., Howie, A., and Whelan, M. J., 1960, Phil. Trans. A 252, 499.

Howie, A., 1960, Phil. Mag. 5, 251.

Kabemoto, S., 1965, Jap. J. App. Phys. 4, 896.

Kino, T., Kabemoto, S., Maeta, H., and Yamagata, T., 1963, J. Phys. Soc. Japan 18, 1846.

Kiritani, M., 1964, J. Phys. Soc. Japan 19, 618.

Kiritani, M., 1965, J. Phys. Soc. Japan 20, 1834.

Kiritani, M., Nishikawa, T. and Yoshida, S., 1969, J. Phys. Soc. Japan 27, 67.

Kiritani, M. and Yoshida, S., 1963, J. Phys. Soc. Japan 18, 915.

Rider, J. G. and Foxon, C. T. B., 1966, Phil. Mag. 13, 289.

Sato, A., Shimomura, Y., Kiritani, M., and Yoshida, S., 1967, J. Phys. Soc. Japan 22, 1198.

Shimomura, Y., 1965, J. Phys. Soc. Japan 20, 965.

Shimomura, Y. and Yoshida, S., 1967, J. Phys. Soc. Japan 22, 319.

Siegel, R. W., 1966a, Phil. Mag. 13, 337, 1966b, Ibid., 13, 359.

Simmons, R. O. and Balluffi, R. W., 1960, Phys. Rev. 117, 62.

Sondheimer, E. H., 1952, Adv. in Phys. 1, 1.

Yoshida, S., Kino, T., Kiritani, M., Kabemoto, S., Maeta, H., and Shimomura, Y., 1963b, J. Phys. Soc. Japan 18, Suppl. II, 98.

Yoshida, S., Kiritani, M., and Shimomura, Y., 1963a, J. Phys. Soc. Japan 18, 175.

Yoshida, S., Kiritani, M., and Shimomura, Y., 1965a, Lattice Defects in Quenched Metals, edited by R. M. J. Cotterill et al., Academic Press, New York, 713.

Yoshida, S., Kiritani, M., and Yamagata, T., 1965b, J. Phys. Soc. Japan 20, 1662.

Ytterhus, J. A. and Balluffi, R. W., 1965, Phil. Mag. 11, 707.

Table 1. Results of a spectrographic analysis of the nominal 99.9999 wt. % pure aluminum specimen material

Impurity element	Ag	Cu	Fe	Mg	Si
Content (at. ppm)	<0.03	0.1	0.5	0.1	0.5

Table 2. Electron microscopy and resistivity data

Specimen #	t_a (hr)	N_s ($\times 10^{13}$ cm^{-3})	d_{rms} (Å)	A_{SF} ($\times 10^{3}$ cm^{-1})	ℓ_{disl} ($\times 10^{9}$ cm^{-2})	$\rho(4.2^{\circ}K)$ ($\times 10^{-9}\Omega$cm)	$\Delta\rho(\infty)$ ($\times 10^{-9}\Omega$cm)	c_v ($\times 10^{-4}$)
1	0	5.3 ± 0.7	1197 ± 59	4.9 ± 0.8	1.90 ± 0.27	1.243	2.43	1.2 ± 0.2
2	5	3.7 ± 0.7	1409 ± 67	4.8 ± 1.0	1.57 ± 0.30	1.435	2.43	1.1 ± 0.2
3	20	3.3 ± 0.7	1564 ± 59	5.3 ± 1.1	1.56 ± 0.31	1.332	1.71	1.2 ± 0.2
4	23	2.9 ± 0.3	1691 ± 56	5.3 ± 0.7	1.46 ± 0.16	1.395	1.79	1.2 ± 0.2
5	36	2.0 ± 0.3	1786 ± 73	4.2 ± 0.7	1.08 ± 0.17	1.329	0.60	1.0 ± 0.2
6	48	1.7 ± 0.3	1595 ± 71	2.8 ± 0.6	0.82 ± 0.16	1.347	1.47	0.7 ± 0.2

FIGURE CAPTIONS

Fig. 1. The measured resistivity ratio, $\rho(20^{\circ}C)/\rho(4.2^{\circ}K)$, plotted as a function of the pre-quench annealing time, t_a. The pre-quench annealing temperature was $T_a = 600^{\circ}C$.

Fig. 2. Representative regions of two specimens annealed at $600^{\circ}C$ for different times, t_a, quenched from $T_Q = 580^{\circ}C$ and aged at $T_A = 40^{\circ}C$ showing the vacancy precipitate structures observed. (a) Specimen 1; $t_a = 0$ h. (b) Specimen 4; $t_a = 23$ h. Double faulted loops are pointed out by arrows.

Fig. 3. The faulted dislocation loop density, N_s, plotted as a function of the pre-quench annealing time, t_a, at $T_a = 600^{\circ}C$. The specimens were quenched from $T_Q = 580^{\circ}C$ and aged at $T_A = 40^{\circ}C$.

Figure 1

Figure 2

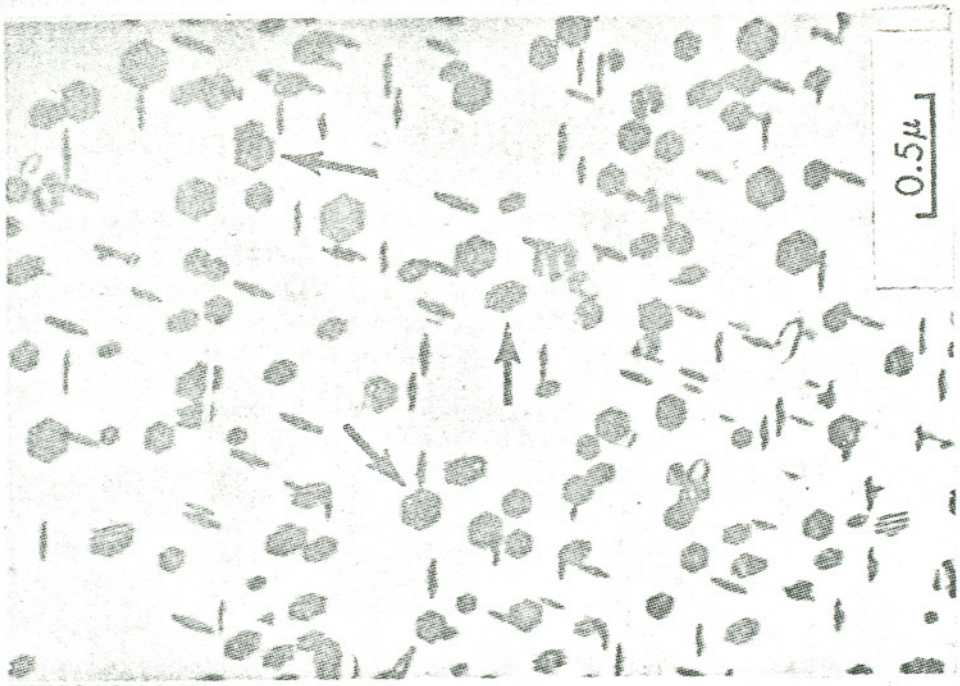

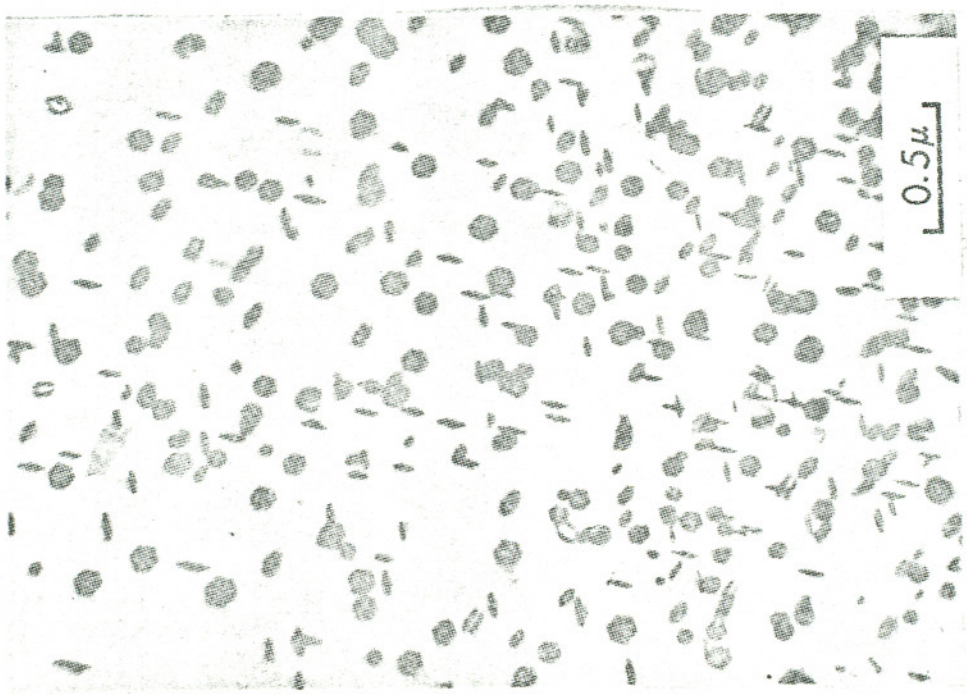

Figure 3